ISSN: 2578-7365

Research Article

Journal of Chemistry: Education Research and Practice

Electromagnetic Interference Shielding Properties of ($Ni_{0.5}Zn_{0.5}Fe_2O_4$/CI/CB) Ternary Composites-Filled Paraffin Wax Matrix

A Houbi[1,2*], AA Zharmenov[1,2], Y Atassi[3], ZT Bagasharova[1,2], S Mirzalieva[1,2], BA Karibayev[4]

[1]National Center on Complex Processing of Mineral Raw Materials of the Republic of Kazakhstan, Almaty, Kazakhstan

[2]Department of Chemical Technology of Inorganic Substances, Al-Farabi Kazakh National University, Almaty, Kazakhstan

[3]Department of Applied Physics, Higher Institute for Applied Sciences and Technology, Damascus, Syria

[4]Department of Physics and Technology, Al-Farabi Kazakh National University, Almaty, Kazakhstan

[*]Corresponding author

A Houbi, National Center on Complex Processing of Mineral Raw Materials of the Republic of Kazakhstan, Almaty, Kazakhstan and Department of Chemical Technology of Inorganic Substances, Al-Farabi Kazakh National University, Almaty, Kazakhstan.

Submitted: 25 Jun 2022; **Accepted**: 04 Jul 2022; **Published**: 26 Oct 2022

Citations: *A, Houbi., AA, Zharmenov., Y, Atassi., ZT, Bagasharova., S, Mirzalieva., et al. (2022). Electromagnetic Interference Shielding Properties of ($Ni_{0.5}Zn_{0.5}Fe_2O_4$/CI/CB) Ternary Composites-Filled Paraffin Wax Matrix, J Chem Edu Res Prac, 6(2), 392-401.*

Abstract

In this work, Ternary composites of NiZn ferrite/carbonyl iron/carbon black ($Ni_{0.5}Zn_{0.5}Fe_2O_4$/CI/CB) are prepared via two stages: Firstly, $Ni_{0.5}Zn_{0.5}Fe_2O_4$ is prepared using a self-combustion method. After that, the process is continued via mixing CB, CI, and $Ni_{0.5}Zn_{0.5}Fe_2O_4$ through the grinding balls. Three various weight ratios of $Ni_{0.5}Zn_{0.5}Fe_2O_4$/CI/CB (1:1:1, 1:1:2, and 2:1:1) with various thicknesses (2–4–6 mm) are prepared. The absorbers are prepared by dispersing ($Ni_{0.5}Zn_{0.5}Fe_2O_4$/CI/CB) composites with a weight ratio of 40% w/w within a paraffin wax matrix. X-ray diffractometry and FTIR spectroscopy are utilized in order to characterize the samples. The morphology of the powders is investigated by SEM. The electromagnetic interference (EMI) shielding properties are measured in the frequency band of 8.8–12 GHz to investigate microwave characterization. Microwave absorption materials (MAMs) show wide absorption bandwidths and reasonable surface density. The maximum shielding efficiency is 21.7 dB at 11.0 GHz for 4 mm thickness of the F/CI/CB-111 composite sample.

Keywords: NiZn Spinel Ferrite, Carbonyl Iron, Carbon Black, Surface Density, Shielding Efficiency

Introduction

In recent decades, EM wave radiation in the high-frequency bands has been considered a disturbing threat for electronic devices because when these EM waves interfere with the input signal for these devices, they produce a noise that is named EMI pollution. Generally, EMI would be regarded as an unwanted result of modern technology that has effects dangerous on human health, intelligent devices, telecommunication devices, and military industries. Consequently, this kind of EMI has become a critical worldwide issue and its alleviation could be accomplished only by utilize of EMI shielding materials. Nowadays, several magnetic loss materials such as hexagonal ferrites, spinel ferrites, and carbonyl iron or dielectric loss materials such as conductive polymers (i.e., polyaniline, polypyrrole) and carbonaceous materials (e.g., carbon black, activated carbon, carbon fibers, graphene) have played a significant role for high-frequency EM wave absorption [1–3]. Nevertheless, the drawbacks involving elevated density, low reflection absorption, and narrow wideband have hugely limited conventional loss materials' workable benefits for EM wave absorption [4–7]. In recent years, MA composites based on carbon, carbonyl iron, and ferrite, have obtained significant concern due to their excellent electrical and ferrimagnetic characteristics. Carbonaceous materials-based composites have pulled in major attention for microwave absorption lately because of the unique structure of carbon-based materials. Carbon black is usually used to fit the requirements of high-effective microwave attenuation materials because of its superior characteristics, for example, high permittivity, high specified surface region, unique electronic conductivity, huge interface, etc. [8, 9]. Carbon black has a unique place in the band of elevated-frequency MAMs. Furthermore, spinel ferrites and carbonyl iron have excellent MA characteristics due to their unique magnetic characteristics. NiZn ferrites and carbonyl iron are considered suitable materials for high-frequency implementations [10, 11]. When NiZn ferrite and carbonyl iron are mixed with carbon black, the MA characteristics of the resultant composite are anticipated to enhance. According to this, $BaF_{e12}O_{19}$/CI absorbers with various powder ratio compositions in the frequency range of 2–18 GHz were successfully prepared by Feng et al. [12]. The single-layer and double-layer absorbers were prepared, and their MA characteristics were studied. The results showed that the double-layer absorber was clearly more than that of the single-layer absorber. Where the reflection loss (RL) for the double-layer absorber was -13 dB in the frequency range (6–18 GHz) and less than -8 dB in the frequency range (2–18 GHz). The thicknesses of the absorbers were 3.6 and 3.7 mm, respectively. On the other hand, Yan et al. prepared a mixture of doped polyaniline (PANI) coated porous structure carbonyl iron powder (CIP) and graphene sheets [13]. The results showed that the absorption bandwidth under -10 dB (BW_{-10dB}) was 4.6 GHz for 2 mm thickness for the composites with 40 wt.% of PANI@ porous CIP and 5 wt.% of Graphene. The results showed that graphene-PANI@ porous CIP was a promising wave absorbing composite material. In addition to that Anh et al. prepared successfully a mixture of CB/$Zn_{0.8}Ni_{0.2}Fe_2O_4$ nanoparticles scattered in a SiO_2 matrix [14]. The impacts of NiZn ferrite nanoparticles in the range of 0–1.75 wt% and various coating thicknesses (1–2.5 mm) on MA performance in the frequency band of 8–12 GHz have been studied. The results indicated that a specimen of 1.5 wt% NiZn ferrite nanoparticles content showed the best MA at 10 GHz. Higher coating thicknesses (1–2.5 mm) showed bigger MA and arrived at a so high absorption for 2 mm thickness. Until now, to the best of our knowledge, no studies have been reported on the EMI shielding and MA properties of composites made up of NiZn ferrite/carbonyl iron/carbon black ($Ni_{0.5}Zn_{0.5}Fe_2O_4$/CI/CB). In this work, a perfect absorber was obtained by incorporating $Ni_{0.5}Zn_{0.5}Fe_2O_4$ and CI (magnetic loss materials) and CB (dielectric loss material) within a paraffin wax matrix. Where we study the effect of different weight ratios of $Ni_{0.5}Zn_{0.5}Fe_2O_4$/CI/CB and its effect on EMI shielding properties. A distinct feature of this work is that NiZn ferrite was synthesized through a self-combustion method using polyvinyl alcohol (PVA) as a chelating agent. After that, the process is continued through mixing and grinding CB, CI, and NiZn ferrite by the grinding balls.

Experiment

Synthesis of NiZn Ferrite, Carbonyl Iron and Carbon Black Powders

Ferrite ($Ni_{0.5}Zn_{0.5}Fe_2O_4$) nanoparticles were prepared by a self-combustion method. $Ni_{0.5}Zn_{0.5}Fe_2O_4$ were synthesized by taking appropriate amounts of nickel(II) nitrate hexahydrate ($Ni(NO_3)_2.6H_2O$), zinc nitrate hexahydrate ($Zn(NO_3)_2.6H_2O$), and iron(III) nitrate nonahydrate ($Fe(NO_3)_3.9H_2O$) were blended together with an aqueous solution of sucrose (2 moles per metal ion) and 1% an aqueous solution of polyvinyl alcohol. The whole mixture was blended totally and heated at 90 °C for 7 h to shape a viscous liquid. The heating process was accompanied by the evolution of brown fumes of NO_2 from the decomposed metal nitrate salts. Then, the mixture was transferred to the furnace for drying for 2 h at 200 °C to obtain a fluffy carbonaceous pyrolyzed mass. After that, the resulting mass was annealed for 4 h at 650 °C to obtain nanoparticles ferrite. Typical images of a prepared ferrite by a self-combustion method are shown in Fig. 1. On the other hand, carbonyl iron and carbon black were purchased from Cabot Corporation Company. The average particle size of carbonyl iron and carbon black powders was measured utilizing the sieve shaker and it was between 10-25 µm and 2–8 µm, respectively. Carbonyl iron and carbon black powders were milled for 12 h at 300 rpm via the grinding balls to obtain fine powders.

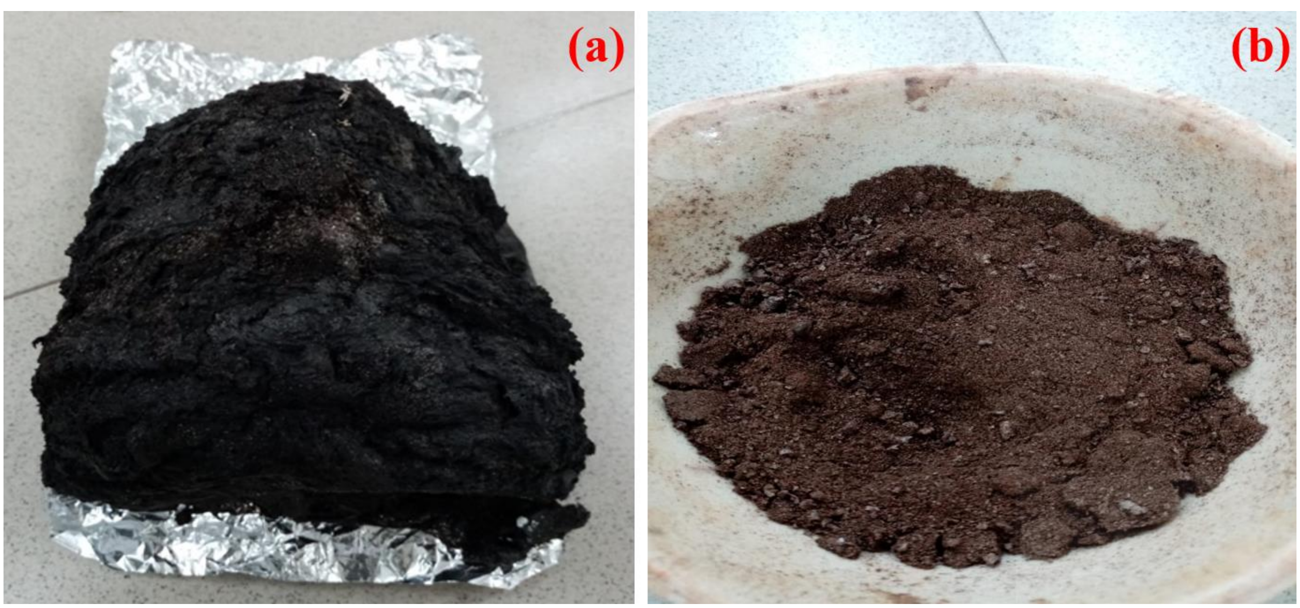

Figure 1: NiZn Ferrite Nanoparticles Prepared by a Self-Combustion Method: (a) Formation of a Fluffy Carbonaceous Pyrolyzed Mass and (b) Obtaining Nanoparticles Ferrite

Synthesis of $Ni_{0.5}Zn_{0.5}Fe_2O_4$/CI/CB Composites

Ferrite nanoparticles were mixed and milled with CI and CB powders by the grinding balls. Three various weight ratios of $Ni_{0.5}Zn_{0.5}Fe_2O_4$/CI/CB (1:1:1, 1:1:2, and 2:1:1) were synthesized. The $Ni_{0.5}Zn_{0.5}Fe_2O_4$/CI/CB composites were milled for 1 h at 300 rpm. Table 1 shows the symbols of composite samples.

Preparation of Absorber Samples

Paraffin wax was symmetrically blended with $Ni_{0.5}Zn_{0.5}Fe_2O_4$/CI/CB composites powders with a weight ratio of 40% w/w within a paraffin wax matrix by heating and stirring for 15 min. Afterward, the single-layer samples were molded to the dimensions of 50×50 mm with various thicknesses (2–4–6 mm) to measure RL and SE in the frequency band of 8.8–12 GHz.

Table 1: Symbols of Composite Samples

Sample symbols	Weight ratio		
	$Ni_{0.5}Zn_{0.5}Fe_2O_4$	CI	CB
F/CI/CB-111	1	1	1
F/CI/CB-112	1	1	2
F/CI/CB-211	2	1	1

Measurements

A powder X-ray diffractometer (XRD, Rigaku Miniflex 600, Cu-Ka) is utilized for defining the crystal structures of the powders. Fourier Transform IR (FTIR) spectra are recorded on a Perkin Elmer spectrum 65 FTIR spectrometer in the range of 400–4000 cm^{-1} A scanning electron microscope (FEI Quanta 200 3D) is utilized for defining the morphology of the powders. The EMI shielding and MA properties of the prepared samples are calculated by using the horn antenna connected to an oscilloscope.

Results and Discussion

XRD Patterns

The crystalline structures of the powders are identified by XRD. The XRD patterns of $Ni_{0.5}Zn_{0.5}Fe_2O_4$, CI and CB powders are shown in Fig. 2. For the $Ni_{0.5}Zn_{0.5}Fe_2O_4$ pattern, nine diffraction peaks are noticed, which conform to (hkl) planes of (111), (220), (311), (222), (400), (422), (511), (440) and (533), respectively. The ideal spinel structure is noticed by the peaks of NiZn ferrite [15]. All the observed peaks of $Ni_{0.5}Zn_{0.5}Fe_2O_4$ are matched with the standard XRD pattern (JCPDS, PDF no. 08–0234). On the other hand, for the carbonyl iron pattern, three characteristic peaks are noticed, which conform to (hkl) planes of (100), (200), and (211), respectively. The XRD pattern of carbonyl iron resembles crystallites in which the sample mainly contains α-Fe phase [16]. All the observed peaks of CI are matched with the standard XRD pattern (JCPDS, PDF no. 06-0696). Finally, for the CB pattern, two characteristic peaks are noticed, which conform to (hkl) planes of (002) and (100), respectively [17].

FTIR Spectra

The FTIR spectra of the $Ni_{0.5}Zn_{0.5}Fe_2O_4$, CI and CB powders is shown in Fig. 3. For the $Ni_{0.5}Zn_{0.5}Fe_2O_4$ nanoparticles, two peaks at 565.4 cm^{-1} and 432.3 cm^{-1} are referring to the stretching vibration of (Fe-O), which emphasizes the formation of the metal-oxygen in ferrite-based [18]. On the other hand, the peak at 1630.4 cm^{-1} in $Ni_{0.5}Zn_{0.5}Fe_2O_4$, CI, and CB is referring to C=O stretching vibration, and the peaks at 2348 cm^{-1} and 3452 cm^{-1} are referring to O-H stretching vibration [19, 20].

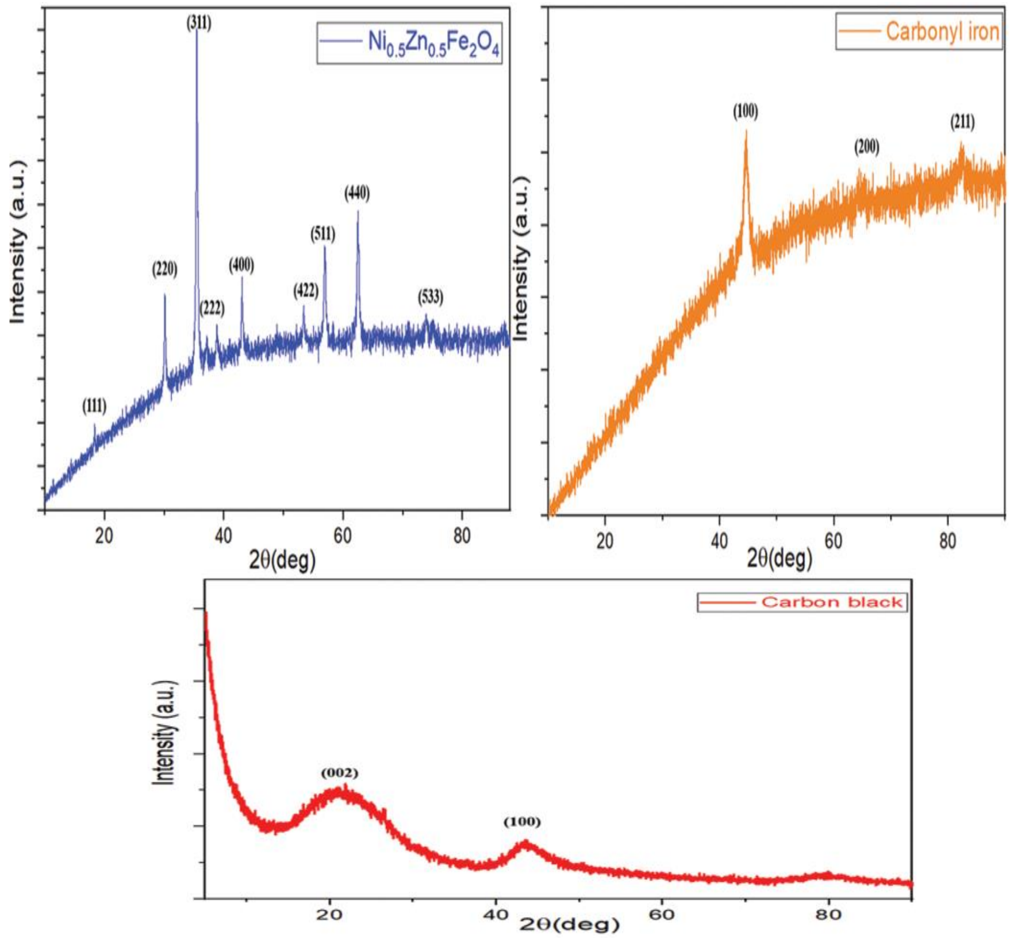

Figure 2: XRD Patterns of $Ni_{0.5}Zn_{0.5}Fe_2O_4$, Carbonyl Iron, and Carbon Black

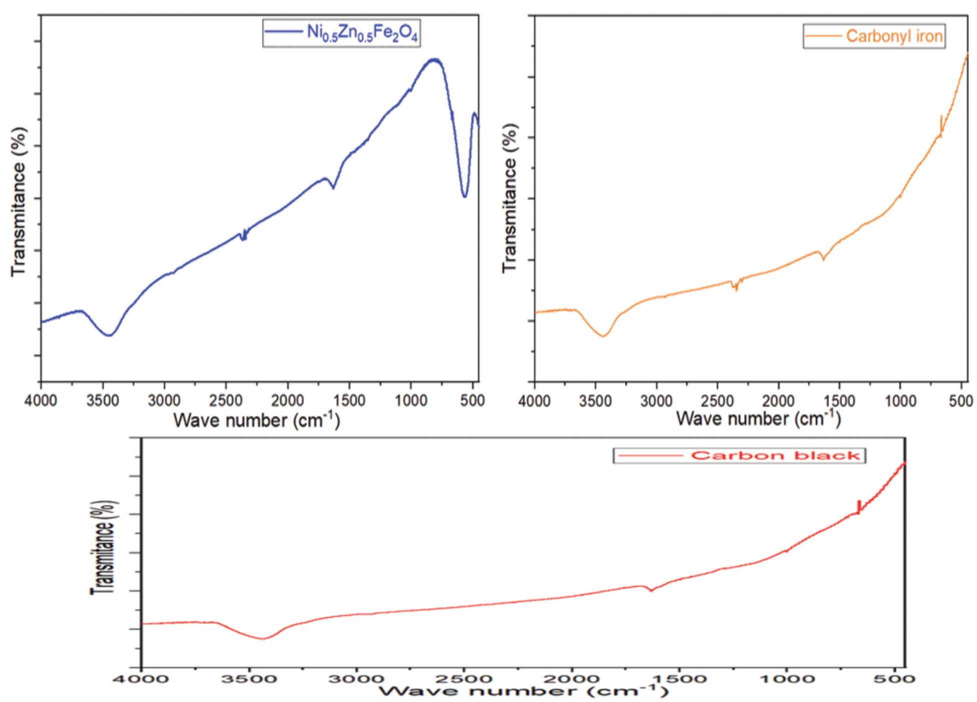

Figure 3: FTIR Spectra of NiZn Ferrite, Carbonyl Iron, and Carbon Black

SEM Analysis

The agglomerated spherical particles of NiZn ferrite and the spherical particles of carbonyl iron (Fig. 4a, b) are observed with the average diameters to be ranging between 18–52 nm and 0.2–2.4 µm, respectively. On the other hand, the average particle size of carbon black powder (Fig. 4c) is noticed to be ranging between 75–481 nm.

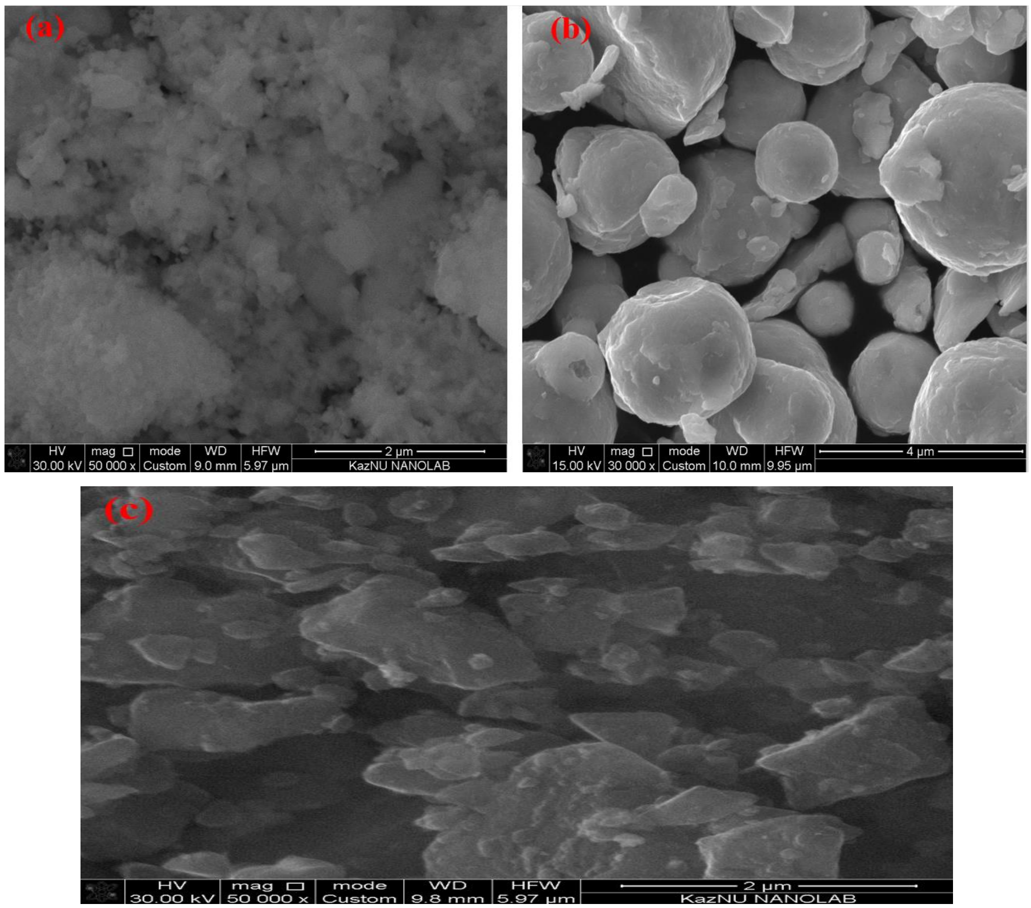

Figure 4: SEM Images of (a) NiZn Ferrite, (b) Carbonyl Iron, and (c) Carbon Black

EMI Shielding Properties

The significant point in EMI shielding is to attenuate the transmitted power of the EM waves (p_T) as shown in Fig. 5. EMI shielding properties of the prepared samples are estimated with the free-space technique as shown in Fig. 6. EM waves are generated by a microwave generator in the frequency band of 8.8–12 GHz (with wavelengths λ= 2.5-3.4 cm), where a microwave generator is connected by a WR90 waveguide instrument (IEC Standard R100, X Band). The incident EM waves (p_{in}) are measured by the horn antenna connected to an oscilloscope (Fig. 6), then the prepared sample perpendicularly is placed between a microwave generator and the horn antenna to measure the transmitted power of the EM waves (p_T) by an oscilloscope. As a result, SE can be calculated for the EMI shielding by applying the equation (1) [21]:

$$SE\ (dB) = SE_R + SE_A + SE_M = 10\ log\frac{p_{in}}{p_T} \quad (1)$$

It is significant to note that the multiple reflection loss (SE_M) can be ignored if the absorption shielding (SE_A) of EMI shielding material is higher than 10 dB and equation (1) then can be rewritten as [21]:

$$SE\ (dB) = SE_R + SE_A = 10\ log\frac{p_{in}}{p_T} \quad (2)$$

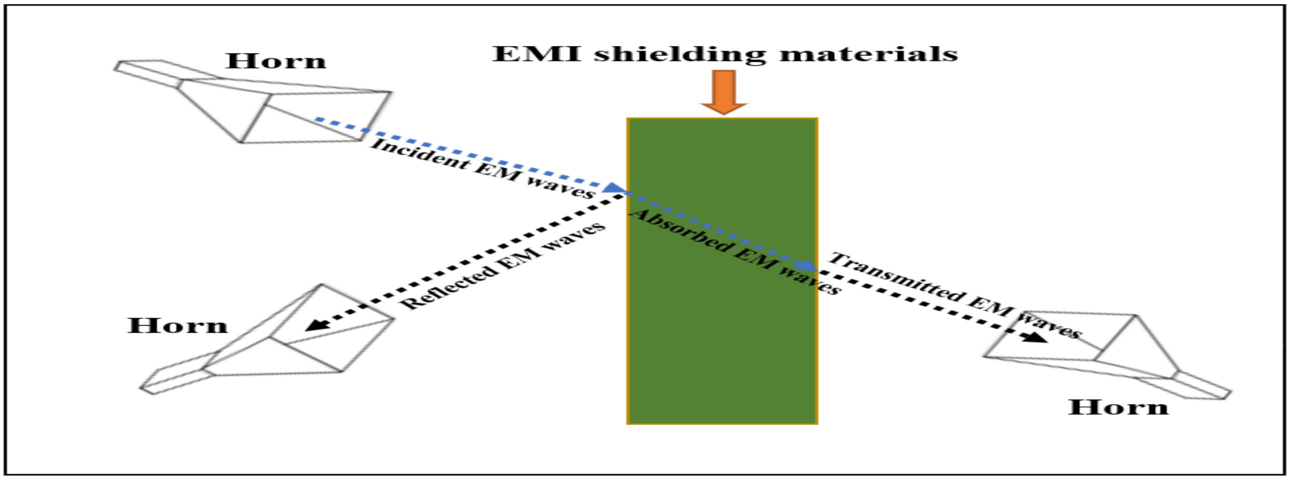

Figure 5: Sketch of the Electromagnetic Interference Shielding Model Used to Measure Shielding Efficiency

In addition to that, the reflected power of the EM waves (p_{ref}) is measured when the EM waves are incident on the sample surface at an angle of 45° by an oscilloscope. As a result, the shielding by reflection (SE_R) can be calculated for the EMI shielding by applying the equation (3).

$$SE_R\ (dB) = -10\log(1-R) = -10\log\left(1-\frac{p_{ref}}{p_{in}}\right) \quad (3)$$

Finally, the shielding by absorption (SE_A) is calculated by equation (4) [22, 23]:

$$SE_A\ (dB) = -10\log\left(\frac{T}{1-R}\right) = -10\log\left(\frac{p_T}{p_{in}-p_{ref}}\right) \quad (4)$$

Fig. 7 represents the shielding efficiency (SE) of F/CI/CB composites in the frequency band of 8.8–12 GHz with various thicknesses (2–4–6 mm). The results illustrate that the maximum shielding efficiency is 21.7 dB at the frequency of 11.0 GHz for the thickness of 4 mm of the F/CI/CB-111 composite sample. Fig. 8 shows the SE_R and SE_A of F/CI/CB composites with various thicknesses (2–4–6 mm) at the frequency of 11.5 GHz.

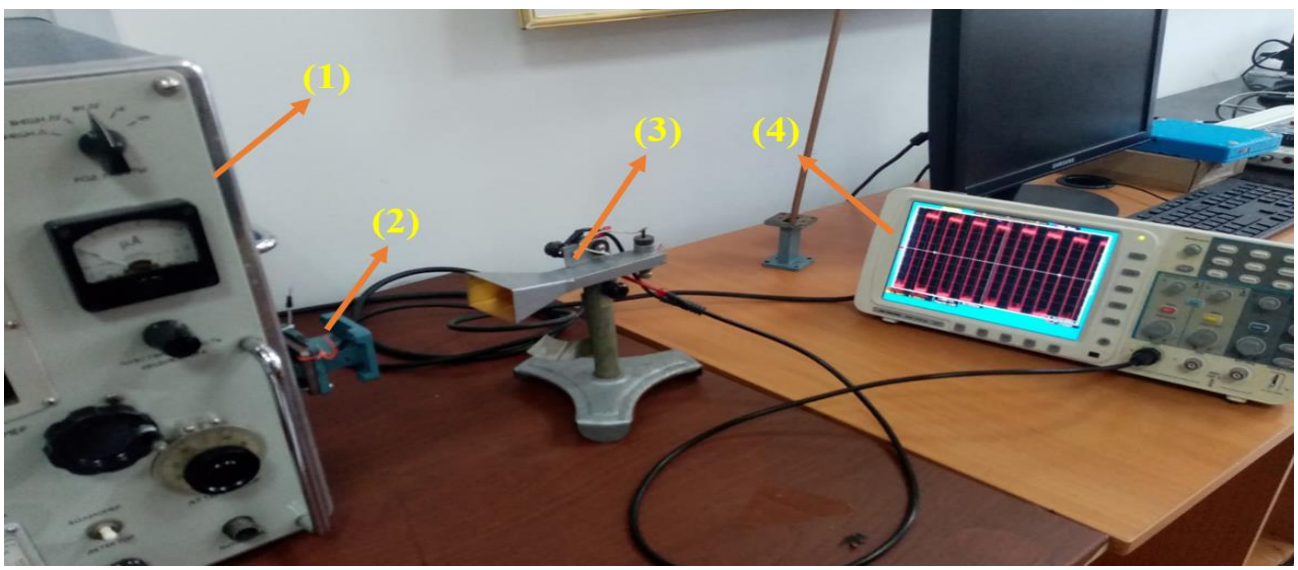

Figure 6: Experimental Setup for Studying the EMI Properties of CB/$Ni_{0.5}Zn_{0.5}Fe_2O_4$ Nanocomposites by the Free-Space Technique. From left to right: (1) Microwave Generator, (2) Waveguide Instrument (IEC Standard R100, X Band), (3) Horn Antenna, and (4) Oscilloscope.

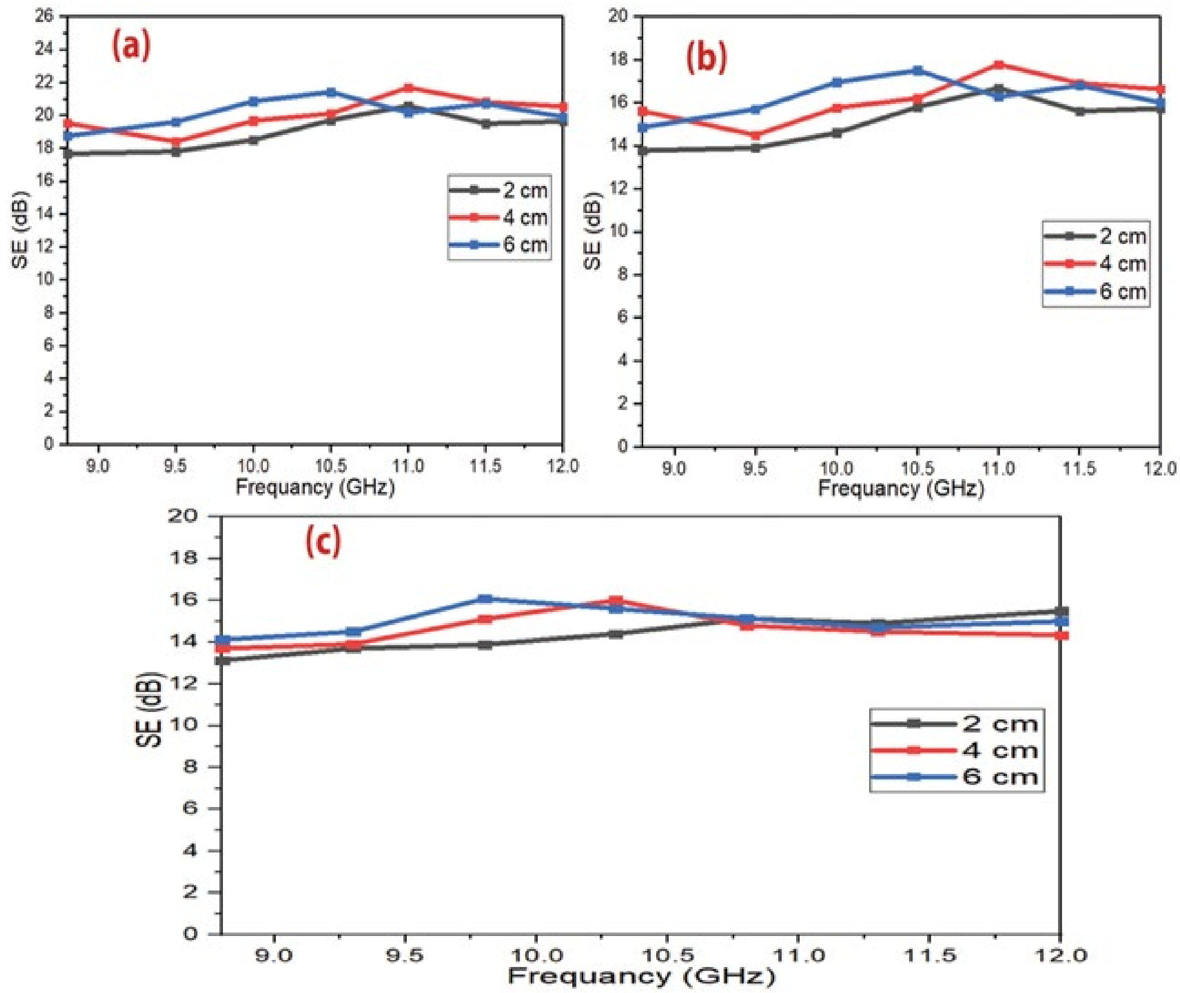

Figure 7: SE Curves of (a) F/CI/CB-111 Composite, (b) F/CI/CB-112 Composite and (c) F/CI/CB-211 Composite at Various Thicknesses (2–4–6 mm).

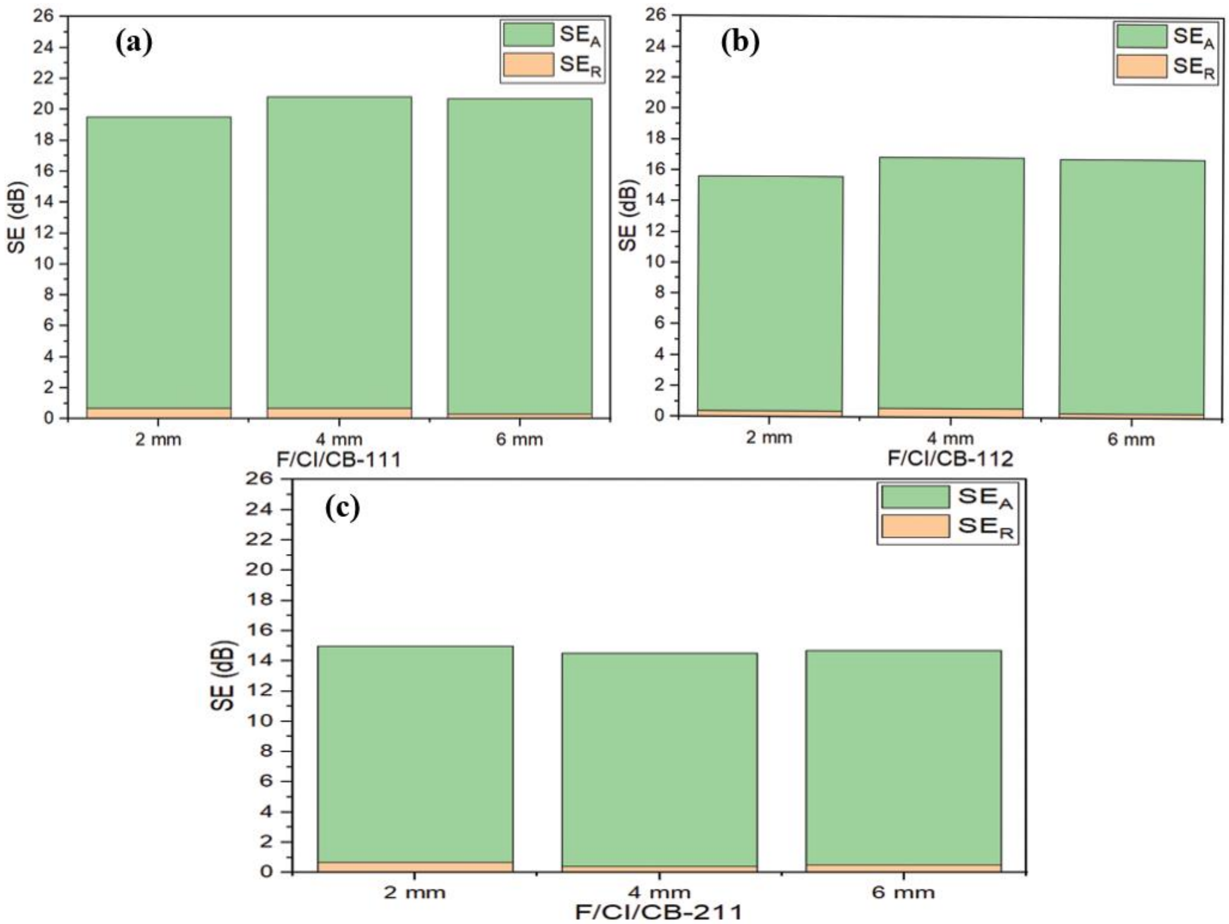

Figure 8: Bar Plot for Individual Components of SER and SEA of (a) F/CI/CB-111 Composite, (b) F/CI/CB-112 Composite and (c) F/CI/CB-211 Composite with Various Thicknesses (2–4–6 mm) at the Frequency of 11.5 GHz.

Table 2 shows the reasonable surface density (SD) of all the prepared absorbers. As a result, one can notice the impact of incorporating $Ni_{0.5}Zn_{0.5}Fe_2O_4$ and CI (magnetic loss materials) and CB (dielectric loss material) on the EMI properties of the prepared absorber.

Table 2: MA Behavior of Ni0.5Zn0.5Fe2O4/CI/CB Composites at Various Thicknesses (2–4–6 mm)

Composite samples	t (mm)	SE (dB)	f (GHz)	SD (kg/m^2)
F/CI/CB-111	2	20.6	11.0	3.86
	4	21.8	10.9	3.87
	6	21.1	10.5	3.89
F/CI/CB-112	2	16.8	10.9	3.62
	4	17.9	11.0	3.64
	6	17.5	10.4	3.65
F/CI/CB-211	2	15.2	11.0	4.01
	4	16.1	10.3	4.02
	6	16.3	10.0	4.04

Conclusion

In the current research, F/CI/CB microwave absorbers were synthesized within a paraffin matrix successfully. F/CI/CB ternary composites were characterized by XRD, FTIR, and SEM. The practical characterization was accomplished by measuring the EMI shielding properties. $Ni_{0.5}Zn_{0.5}Fe_2O_4$ and CI were used to enhance the mechanism of magnetic loss, while CB was introduced to enhance the mechanism of dielectric loss. As a result, one can notice the impact of combining $Ni_{0.5}Zn_{0.5}Fe_2O_4$, CI and CB on the EMI properties of the absorber. Absorbers show wide bandwidths and reasonable surface density. The maximum SE was 21.7 dB at 11.0 GHz for 4 mm thickness of the F/CI/CB-111 composite sample.

Acknowledgments

The authors express their gratitude to Al-Farabi Kazakh National University, the center of complex processing of mineral raw materials, and the center of physical-chemical methods of research and analyses for providing the materials and equipment to conduct this research project.

References

1. Yin, J., Xu, X., Ji, J., Li, X., & Cheng, X. (2022). Synthesis and microwave absorption properties of Fe3O4/CuS composites. physica status solidi (a), 2200189.
2. Houbi, A., Atassi, Y., Zharmenov, A. A., Bagasharova, Z. T., Myrzalieva, S. K., Kadyrakunov, K. B., & Karibayev, B. A. (2022). mr Microwave absorption and electromagnetic interference shielding properties of carbon black/MnNiZn ferrite nanocomposites-filled paraffin wax in the frequency range (8.8–12 GHz). Вестник. Серия Физическая (ВКФ), 81(2), 85-95.
3. Houbi, A., Aldashevich, Z. A., Atassi, Y., Telmanovna, B. Z., Saule, M. (2022). Nanoparticles Coated with Polyaniline Within Paraffin Wax Matrix. 5, 436-448.
4. Liu, Y., Liu, X., & Wang, X. (2015). Synthesis and microwave absorption properties of Ni–Zn–Mn spinel ferrites. Advances in Applied Ceramics, 114(2), 82-86.
5. Adi, W. A., Yunasfi, Y., Mashadi, M., Winatapura, D. S., Mulyawan, A., Sarwanto, Y., & Taryana, Y. (2019). Metamaterial: Smart magnetic material for microwave absorbing material. Electromagnetic Fields and Waves, 1-18.
6. Liu, P. J., Yao, Z. J., Ng, V. M. H., Zhou, J. T., Yang, Z. H., & Kong, L. B. (2018). Enhanced microwave absorption properties of double-layer absorbers based on spherical NiO and Co0. 2Ni0. 4Zn0. 4Fe2O4 ferrite composites. Acta Metallurgica Sinica (English Letters), 31(2), 171-179.
7. Indrusiak, T., Pereira, I. M., Heitmann, A. P., Silva, J. G., Denadai, Â. M., & Soares, B. G. (2020). Epoxy/ferrite nanocomposites as microwave absorber materials: effect of multilayered structure. Journal of Materials Science: Materials in Electronics, 31(16), 13118-13130.
8. Mondal, K., Balasubramaniam, B., Gupta, A., Lahcen, A. A., & Kwiatkowski, M. (2019). Carbon nanostructures for energy and sensing applications. Journal of Nanotechnology, 2019.
9. Kwiatkowski, M., Policicchio, A., Seredych, M., & Bandosz, T. J. (2016). Evaluation of CO2 interactions with S-doped nanoporous carbon and its composites with a reduced GO: Effect of surface features on an apparent physical adsorption mechanism. Carbon, 98, 250-258.
10. Ting, T. H., Yu, R. P., & Jau, Y. N. (2011). Synthesis and microwave absorption characteristics of polyaniline/NiZn ferrite composites in 2–40 GHz. Materials Chemistry and Physics, 126(1-2), 364-368.
11. Houbi, A., Aldashevich, Z. A., Atassi, Y., Telmanovna, Z. B., Saule, M., & Kubanych, K. (2021). Microwave absorbing properties of ferrites and their composites: A review. Journal of Magnetism and Magnetic Materials, 529, 167839.
12. Feng, W., Cao, Y., Gang, J., & Su, W. (2018). Preparation and microwave absorption property of BaFe12-xTixO19/carbonyl iron powder nanocomposites. Integrated Ferroelectrics, 190(1), 63-70.
13. Yan, Y. Q., Cai, H. P., Liao, Z. Q., & Xiao, H. B. (2018). Microwave absorption properties of absorber based on polyaniline coated porous carbonyl iron powder and graphene sheets/epoxy composites. Dig. J. Nanomater. Biostruct., 13(1), 107-114.
14. Anh, L. T. Q., & Van Dan, N. (2020). A microwave-absorbing property of super-paramagnetic zinc–nickel ferrite nanoparticles in the frequency range of 8–12 GHz. Applied Physics A, 126(1), 1-6.
15. El Nahrawy, A. M., Salah El-Deen, H., Soliman, A. A., & Mosa, W. M. (2019). Crystallographic and magnetic properties of Al3+ co-doped NiZnFe2O4 nano-particles prepared by sol-gel process. Egyptian Journal of chemistry, 62(3), 525-532.
16. Bahri-Laleh, N., Didehban, K., Yarahmadi, E., Mirmohammadi, S. A., & Wang, G. (2018). Microwave absorption properties of polyaniline/carbonyl iron composites. Silicon, 10(4), 1337-1343.
17. Hu, E., Hu, X., Liu, T., Fang, L., Dearn, K. D., & Xu, H. (2013). The role of soot particles in the tribological behavior of engine lubricating oils. Wear, 304(1-2), 152-161.
18. Kondawar, S. B., & Nandapure, A. I. (2014). Magnetic and electrical properties of zinc-substituted nickel ferrite reinforced conducting polyaniline nanocomposites. Journal of the Chinese Advanced Materials Society, 2(3), 186-198.
19. Ramírez, S. F., & Miranda-Hernández, M. (2012). Carbon film electrodes as support of metallic particles. Int. J. Electrochem. Sci, 7(1), 150-166.
20. Kim, S. Y., Kwon, S. H., Liu, Y. D., Lee, J. S., You, C. Y., & Choi, H. J. (2014). Core–shell-structured cross-linked poly (glycidyl methacrylate)-coated carbonyl iron microspheres and their magnetorheology. Journal of Materials Science, 49(3), 1345-1352.
21. Verma, P., Bansala, T., Chauhan, S. S., Kumar, D., Deveci, S., & Kumar, S. (2021). Electromagnetic interference shielding performance of carbon nanostructure reinforced, 3D printed polymer composites. Journal of Materials Science, 56(20),

11769-11788.
22. Bayat, M., Yang, H., Ko, F. K., Michelson, D., & Mei, A. (2014). Electromagnetic interference shielding effectiveness of hybrid multifunctional Fe3O4/carbon nanofiber composite. Polymer, 55(3), 936-943.
23. Hong, Y. K., Lee, C. Y., Jeong, C. K., Lee, D. E., Kim, K., & Joo, J. (2003). Method and apparatus to measure electromagnetic interference shielding efficiency and its shielding characteristics in broadband frequency ranges. Review of scientific instruments, 74(2), 1098-1102.